Hartree-Fock-Bogoliubov (HFB) theory

General remarks

- HF + BCS theory: mean field and pairing are decoupled.

BCS pairing is added to HF mean field calculations (fairly trivial modification: replace HF occupation numbers by those of BCS). This approach works well near the valley of stability.

- HFB theory: mean field and pairing field influence each other.

Self-consistent theory of both phenomena. Start from generalized variational principle. Canonical transformation (Bogoliubov) to "quasi-particles".
This approach is essential for nuclei far away from stability.

HFB formalism: quasi-particle transformation

Creation operators for nucleon states: $\hat{c}_i^\dagger$

$$\hat{H} = \sum_{i,j=1}^{\infty} \langle i|t|j\rangle \hat{c}_i^\dagger \hat{c}_j + \frac{1}{2} \sum_{i,j,k,l=1}^{\infty} \langle ij|V^{(2)}|kl\rangle \hat{c}_i^\dagger \hat{c}_j^\dagger \hat{c}_l \hat{c}_k$$

$$+ \frac{1}{6} \sum_{i,j,k,l,m,n=1}^{\infty} \langle ijk|V^{(3)}|lmn\rangle \hat{c}_i^\dagger \hat{c}_j^\dagger \hat{c}_k^\dagger \hat{c}_n \hat{c}_m \hat{c}_l$$

Canonical transformation to quasi-particles: $\hat{\beta}_k$

ground state = quasiparticle vacuum

$$\begin{pmatrix} \hat{\beta} \\ \hat{\beta}^\dagger \end{pmatrix} = \begin{pmatrix} U^\dagger & V^\dagger \\ V^T & U^T \end{pmatrix} \begin{pmatrix} \hat{c} \\ \hat{c}^\dagger \end{pmatrix}$$

$$\hat{\beta}_k |\Phi_0\rangle = 0$$

HFB energy density functional and generalized variational principle

$$E'(R) = \langle \Phi_0 | \hat{H} - \hat{N}\lambda | \Phi_0 \rangle$$

Generalized density matrix

Lagrange multiplier (Fermi energy)

Variational principle yields HFB wave equations

$$\delta|_R \left[E'(R) - trace\left\{ \Lambda \left(R^2 - R \right) \right\} \right] = 0$$

Lagrange multiplier

groundstate = quasiparticle vacuum

HFB equations for quasi-particle wave functions (in coordinate space)

$$\begin{pmatrix} (h-\lambda) & \tilde{h} \\ \tilde{h} & -(h-\lambda) \end{pmatrix} \begin{pmatrix} \phi_\alpha^{(1)} \\ \phi_\alpha^{(2)} \end{pmatrix} = E_\alpha \begin{pmatrix} \phi_\alpha^{(1)} \\ \phi_\alpha^{(2)} \end{pmatrix}$$

Mean-field Hamiltonian

$$h = \begin{pmatrix} h_{\uparrow\uparrow}(\vec{r}) & h_{\uparrow\downarrow}(\vec{r}) \\ h_{\downarrow\uparrow}(\vec{r}) & h_{\downarrow\downarrow}(\vec{r}) \end{pmatrix}$$

Pairing-field Hamiltonian

$$\tilde{h} = \begin{pmatrix} \tilde{h}_{\uparrow\uparrow}(\vec{r}) & \tilde{h}_{\uparrow\downarrow}(\vec{r}) \\ \tilde{h}_{\downarrow\uparrow}(\vec{r}) & \tilde{h}_{\downarrow\downarrow}(\vec{r}) \end{pmatrix}$$

two types of spinor wave functions

$$\phi_\alpha^{(1)} = \begin{pmatrix} \phi_\alpha^{(1)}(\vec{r},\uparrow) \\ \phi_\alpha^{(1)}(\vec{r},\downarrow) \end{pmatrix} \qquad \phi_\alpha^{(2)} = \begin{pmatrix} \phi_\alpha^{(2)}(\vec{r},\uparrow) \\ \phi_\alpha^{(2)}(\vec{r},\downarrow) \end{pmatrix}$$

HFB particle density and pairing density in terms of quasi-particle wave functions

$$\rho_q(\vec{r}) = \sum_{\alpha} \sum_{\sigma=\uparrow\downarrow} \left|\phi_{\alpha}^{(2)}(\vec{r}\, q\, \sigma)\right|^2$$

normal density

$$\tilde{\rho}_q(\vec{r}) = -\sum_{\alpha} \sum_{\sigma=\uparrow\downarrow} \phi_{\alpha}^{(2)}(\vec{r}\, q\, \sigma)\, \phi_{\alpha}^{(1)*}(\vec{r}\, q\, \sigma)$$

pairing density

Observables predicted by HFB theory

Same as in HF theory, but in addition:

- Pairing density distribution of protons and neutrons

⇒ pairing energy for p / n

⇒ average pairing gap for p / n

- quasi-particle energy spectrum (and equivalent s.p. energy spectrum)

NOTE: HFB is a ground state theory.

For excited states we need Quasi-particle Random Phase Approximation = QRPA

HFB codes in coordinate space

- 1-D radial grid (for spherical nuclei)
  Dobaczewski, Flocard & Treiner, Nucl. Phys. A422, 103 (1984)

- 3-D Cartesian lattice, diagonalize HFB in HF basis
  maximum continuum energy is quite small (5 MeV)
  Terasaki, Heenen, Flocard & Bonche, Nucl. Phys. A600, 371 (1996)

- 2-D grid (axial), HFB in "transformed harmonic oscillator" (THO) basis
  Stoitsov, Dobaczewski, Ring & Pittel, Phys. Rev. C61, 034311 (2000)

- 2-D grid (axial), HFB in B-Spline representation
  VU group: Oberacker, Umar, Teran, Blazkiewicz (2003-2007)

- 2-D grid (axial), HFB in B-Spline representation
  Pei, Stoitsov, Fann, Nazarewicz, Schunck & Xu, Phys. Rev. C78, 064306 (2008)

Comparison of calculated binding energies with experimental data

HF / HFB calculations use Skyrme (SLy4) interaction + delta pairing interaction

Binding energies [MeV]

Nucleus	HF + BCS/LN (2D)	HFB (2D)	Exp.
^{24}O	-173.76	-172.47	-168.96
^{96}Zr	-828.44	-826.91	-829.00
^{124}Sn	-1050.39	-1049.75	-1049.96

Note: none of the above nuclei are used in the Skyrme (SLy4) force fit!

Stable nucleus ^{16}O
HFB-2D calculation, SLy4 N-N interaction

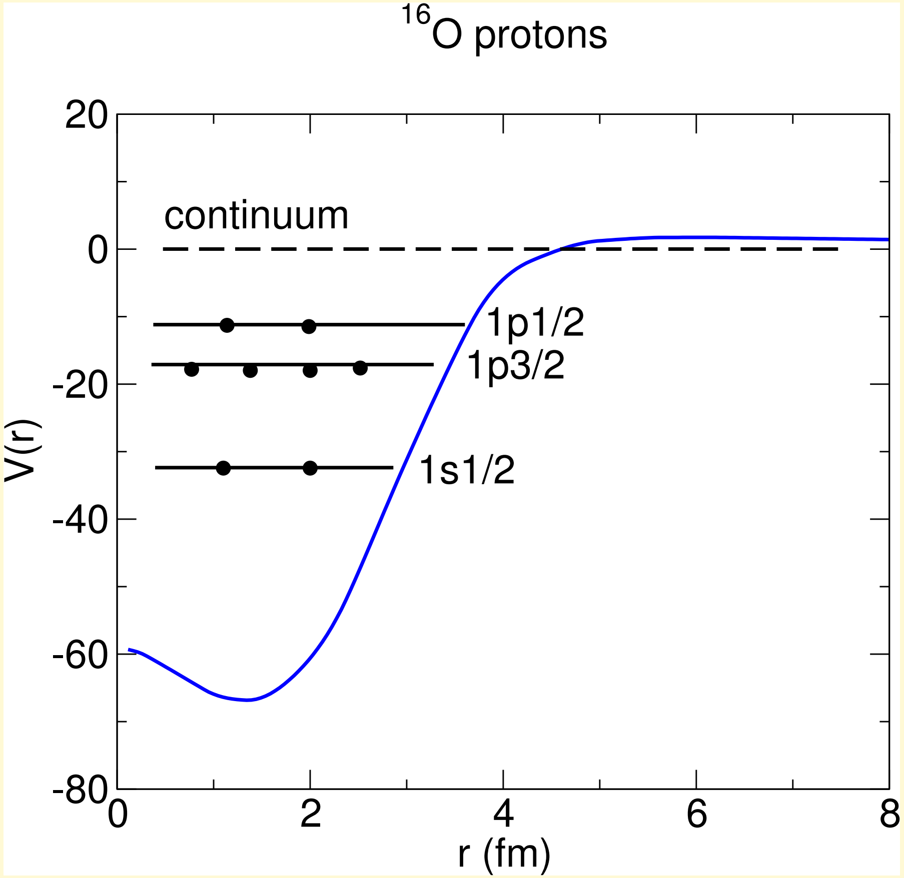

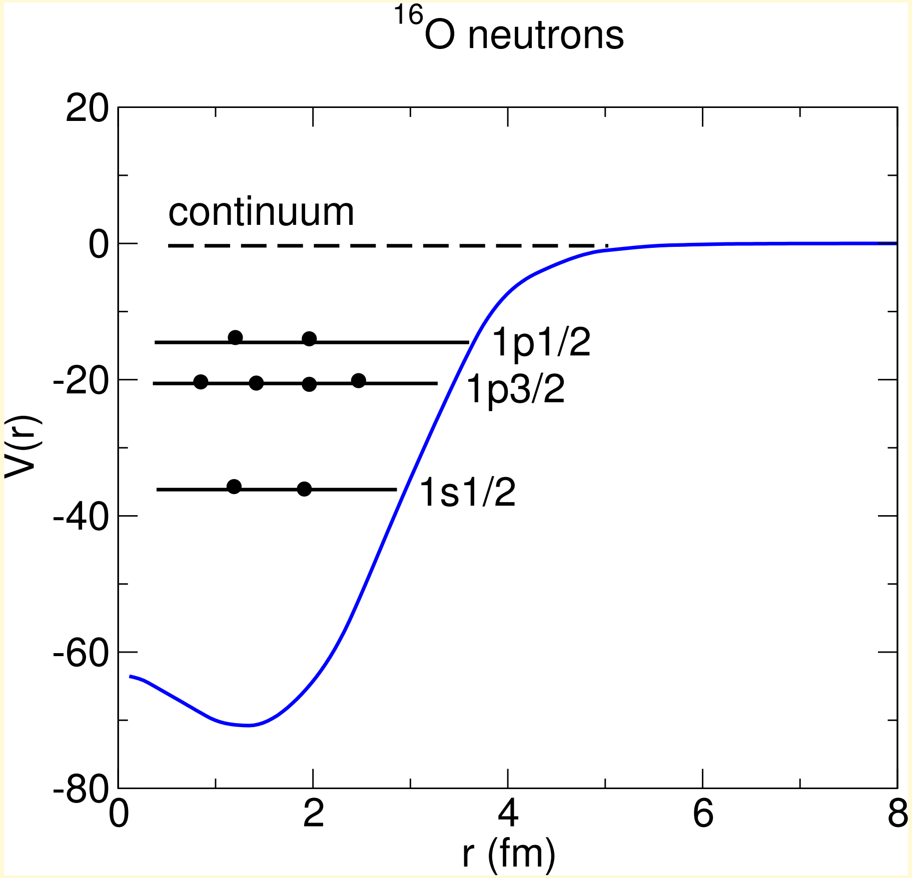

Neutron dripline nucleus ^{24}O ($T_{1/2}$ = 65 ms)
HFB-2D calculation, SLy4 N-N interaction

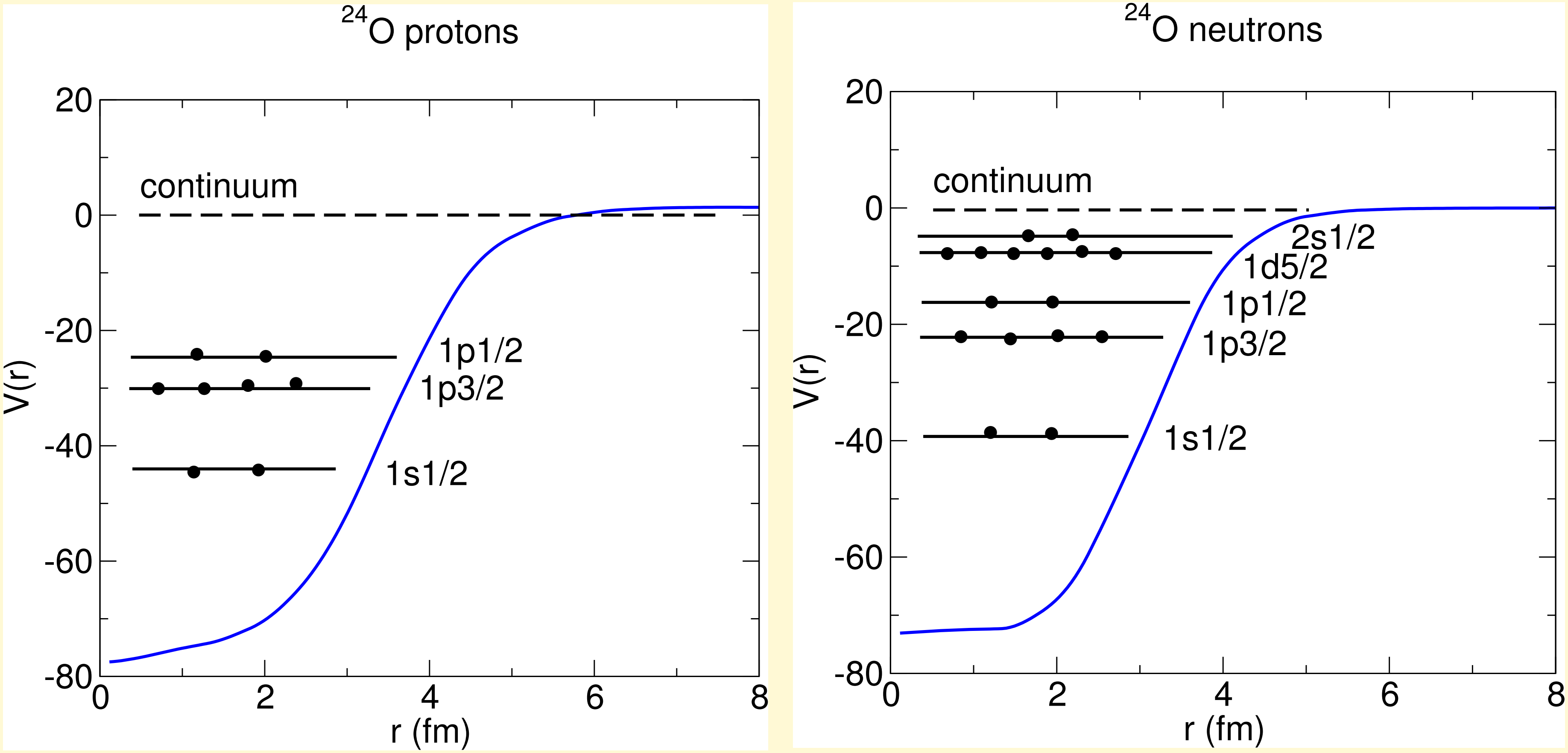

2n-dripline nucleus ^{122}Zr (Z=40, N=82), HFB-2D, SLy4

Artur Blazkiewicz, Ph.D. thesis results (2005)

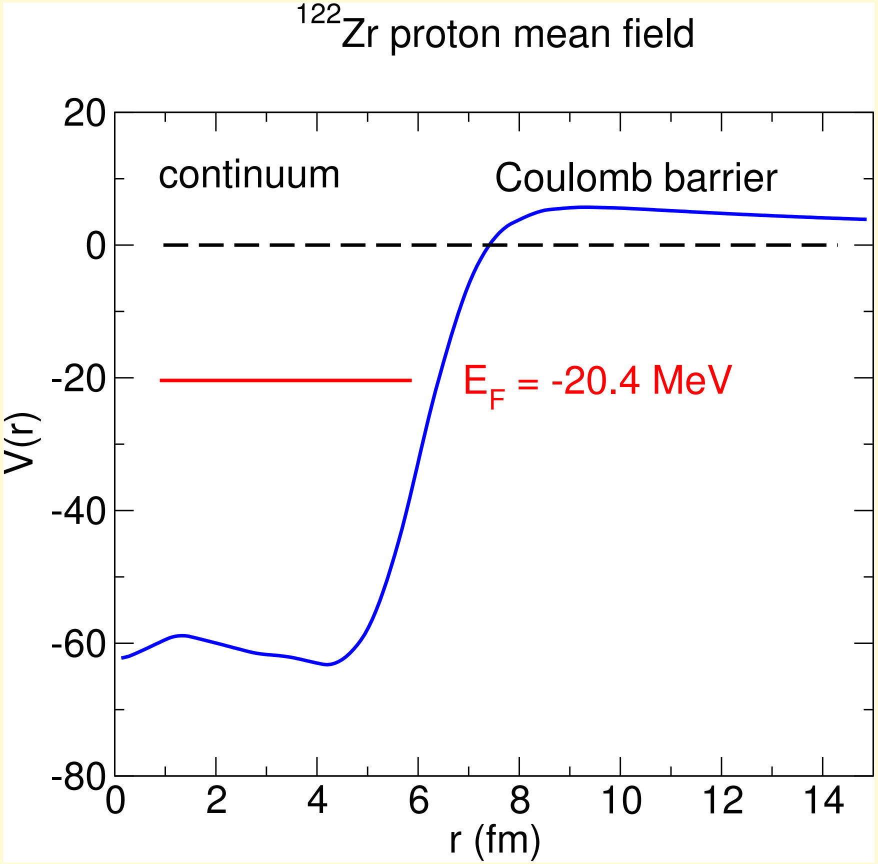

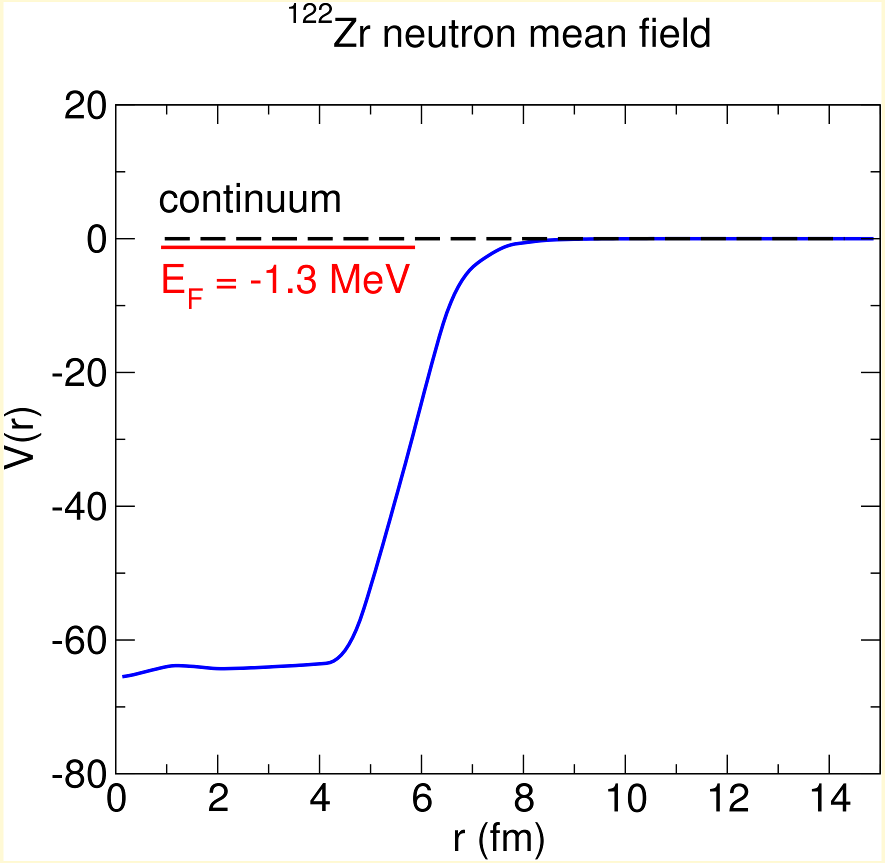

Neutrons at Fermi energy are almost unbound. Neutron wave functions spread out much more than those of protons: "neutron skin"

HFB in coordinate space (2-D / 3-D lattice)

Computational Challenges near neutron-dripline

3 types of wavefunctions

- well-bound states
- weakly-bound states
- continuum states

Other features

- strong pairing correlations for nuclei near neutron dripline
- strong continuum coupling

For nuclei near the neutron dripline, we need accurate solution of HFB continuum problem on coordinate-space lattice, for single-particle energies up to 60 MeV, or even higher for collective excited states via QRPA

Strong continuum coupling near the neutron dripline

Matsuo & Nakatsukasa, Journal of Physics G, May 2010

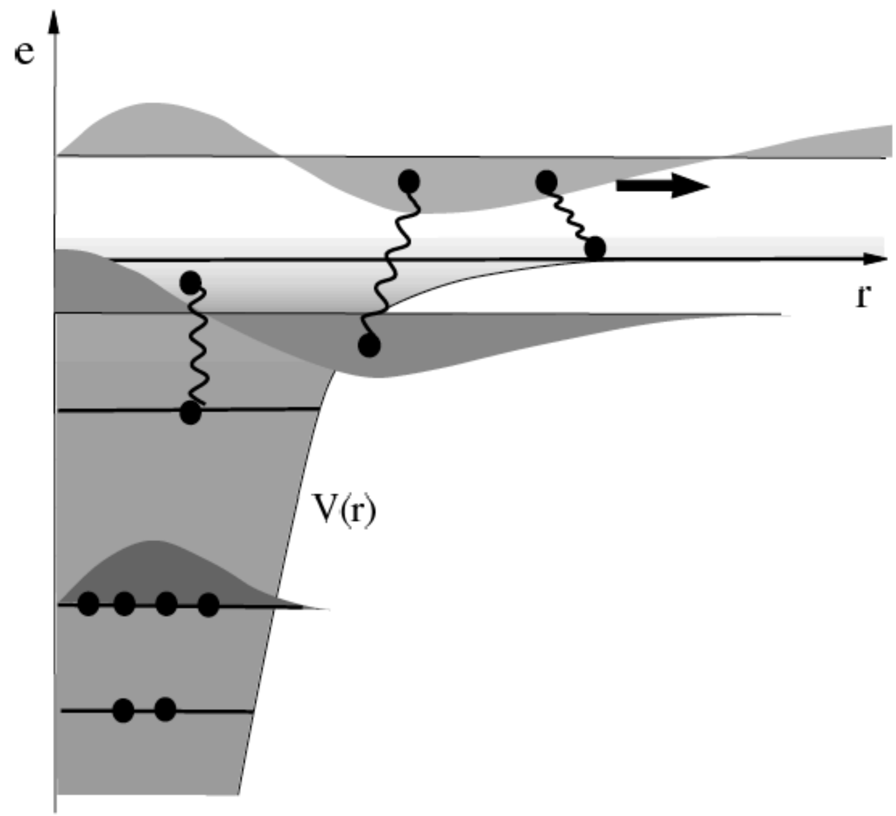

Figure 2. Schematic picture depicting correlations in nuclei near the drip-line, for which correlations involving the loosely bound and unbound continuum orbits play essential roles.

New physics near the neutron dripline

- strong pairing correlations (HF+BCS becomes unrealistic,
  need full HFB)

- highly asymmetric Fermi levels (-20 MeV for protons,
  -1 MeV for neutrons)

- weakly bound neutron states near Fermi level
  neutron halos / neutron skins → neutron star physics!
  strong continuum coupling of weakly bound neutrons

- reduced LS coupling → disappearance of shell gaps
  → abundance of elements created via r - process (Supernovae)

- new collective modes (“pygmy” resonance, “scissors” vibrations, …)

^{102}Zr: normal density and pairing density
HFB, 2-D lattice, SLy4 + volume pairing

Artur Blazkiewicz, Vanderbilt, Ph.D. thesis (2005)

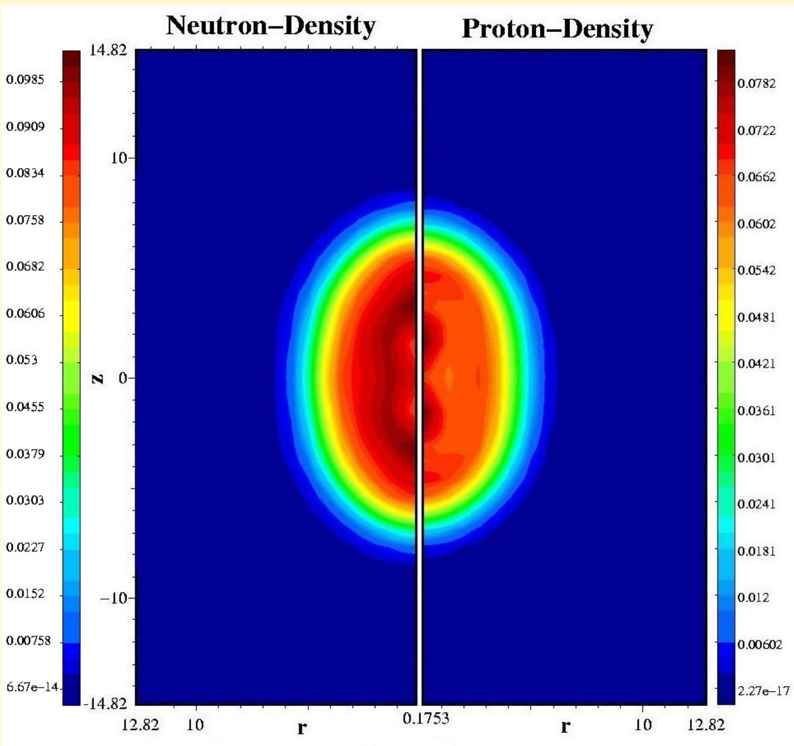

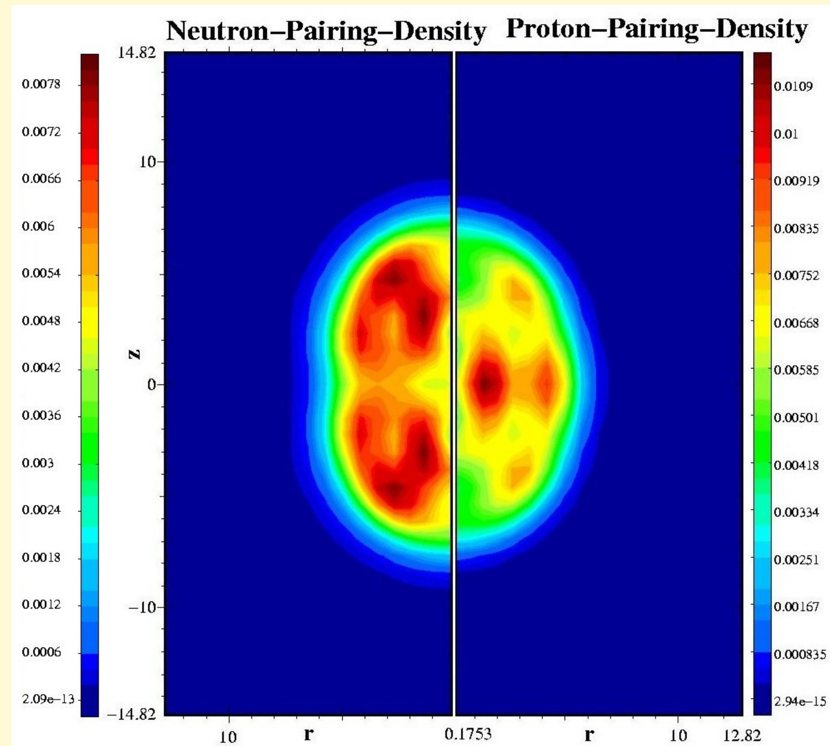

HFB: $\beta_2^{(p)}$=0.43

exp: $\beta_2^{(p)}$=0.42(5) , J.K. Hwang et al., Phys. Rev. C (2006)

^{110}Zr (Z=40, N=70), HFB on 2-D grid

Blazkiewicz, Oberacker, Umar & Stoitsov, Phys. Rev. C71, 054321 (2005)

neutron density | neutron pairing density

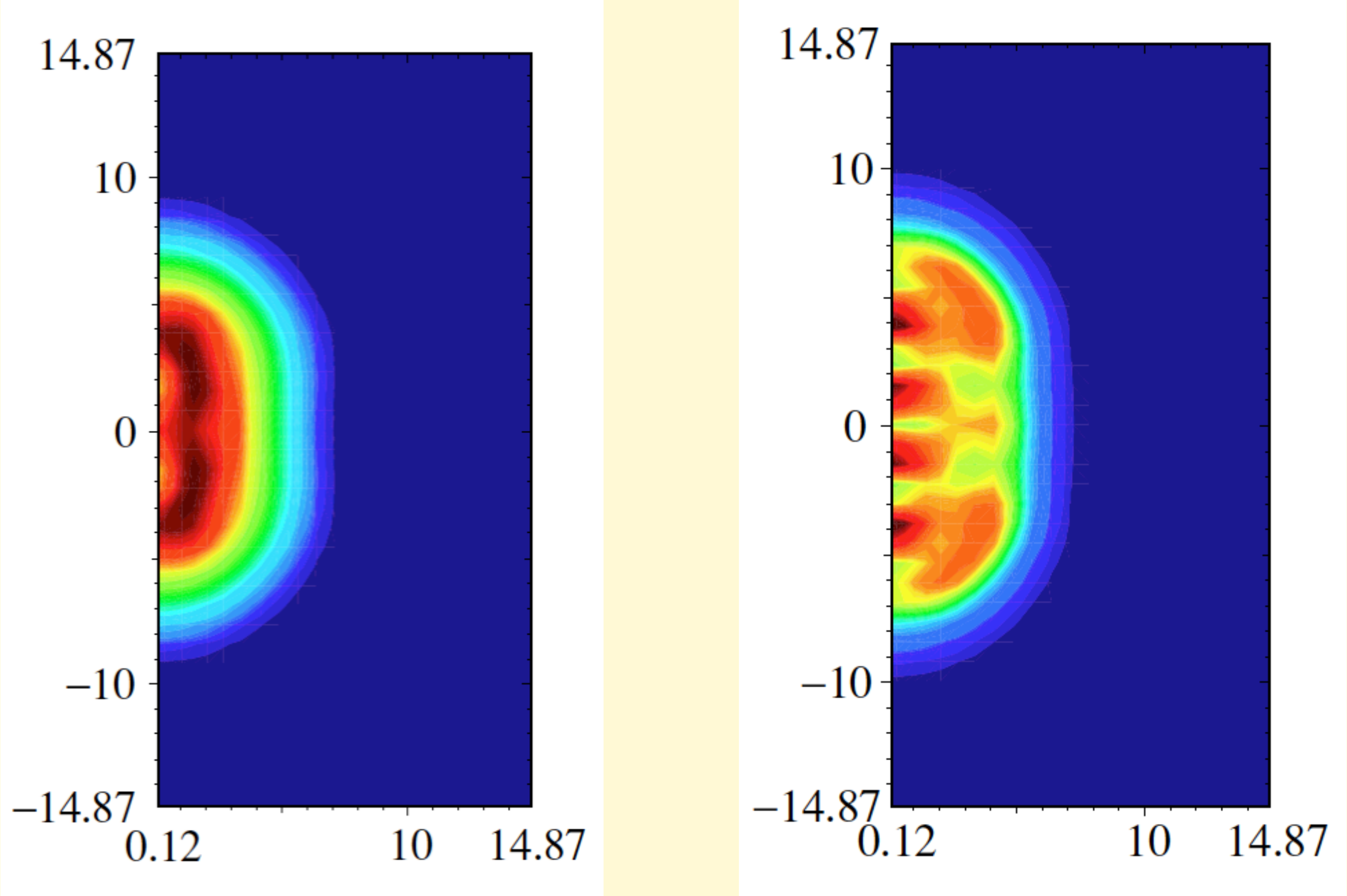

^{104}Zr (Z=40, N=64), HFB on 2D lattice
neutron pairing density: single-particle energy spectrum

Oberacker et al., Proc. NENS03 conference (Niigata, Japan, Nov. 2003)

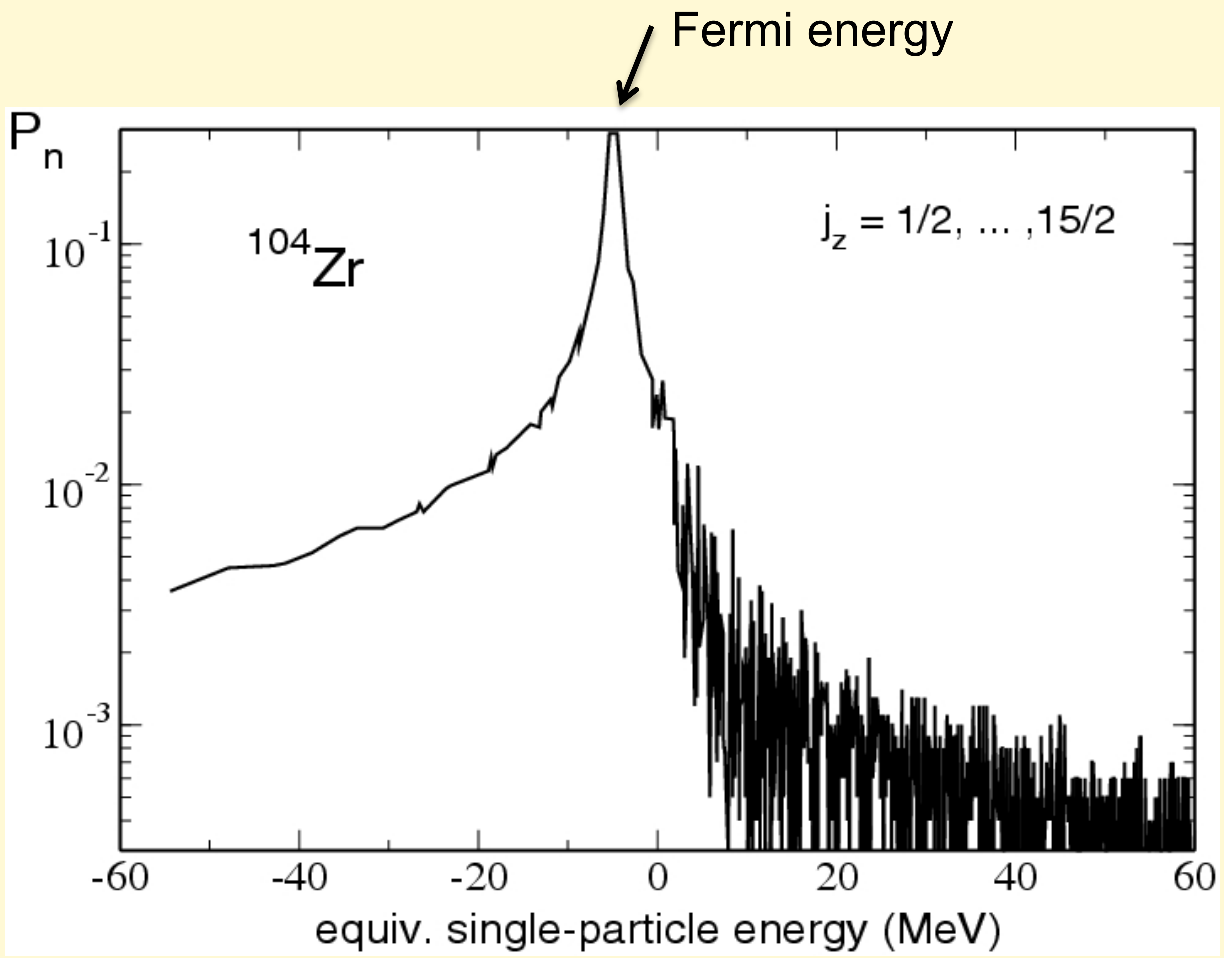

Zirconium isotopes (Z=40), HFB+SLy4 on 2D-grid

Blazkiewicz, Oberacker, Umar & Stoitsov, Phys. Rev. C71, 054321 (2005)

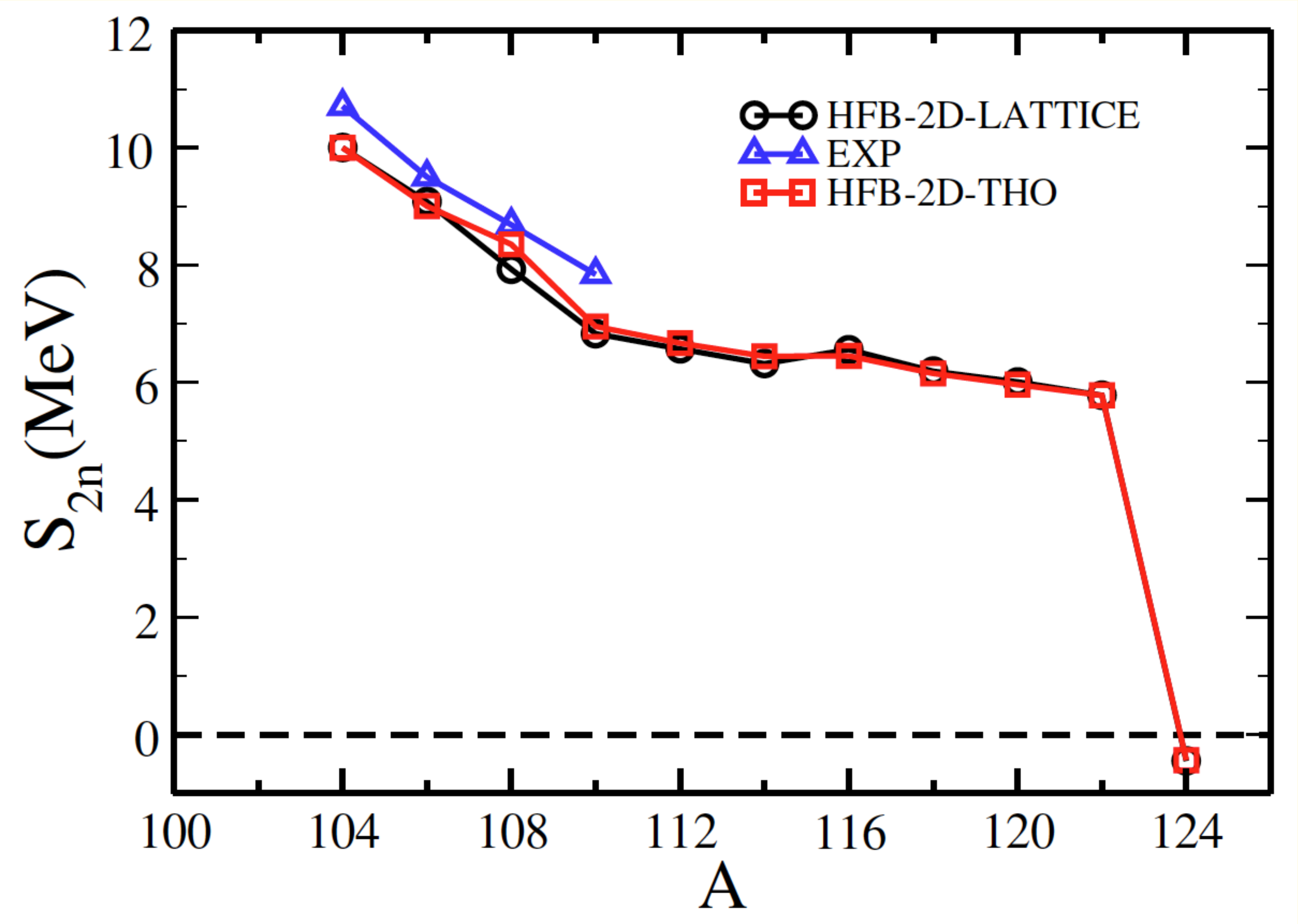

2n-dripline nucleus ^{122}Zr (Z=40, N=82), HFB on 2-D grid

Blazkiewicz, Oberacker, Umar & Stoitsov, Phys. Rev. C71, 054321 (2005)

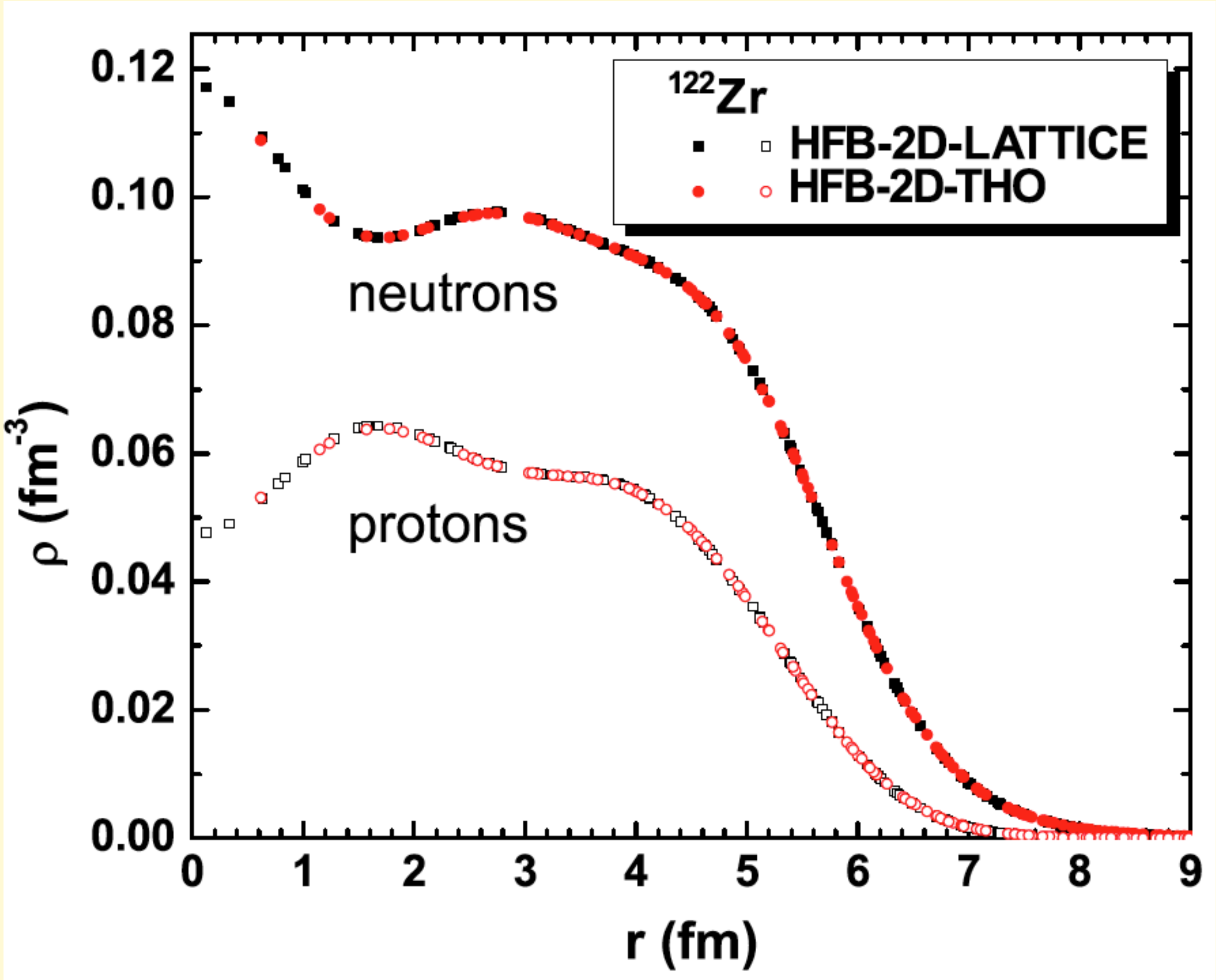

Average neutron pairing gap for zirconium isotopes (Z=40)
HFB-2D (SLy4 + volume pairing)

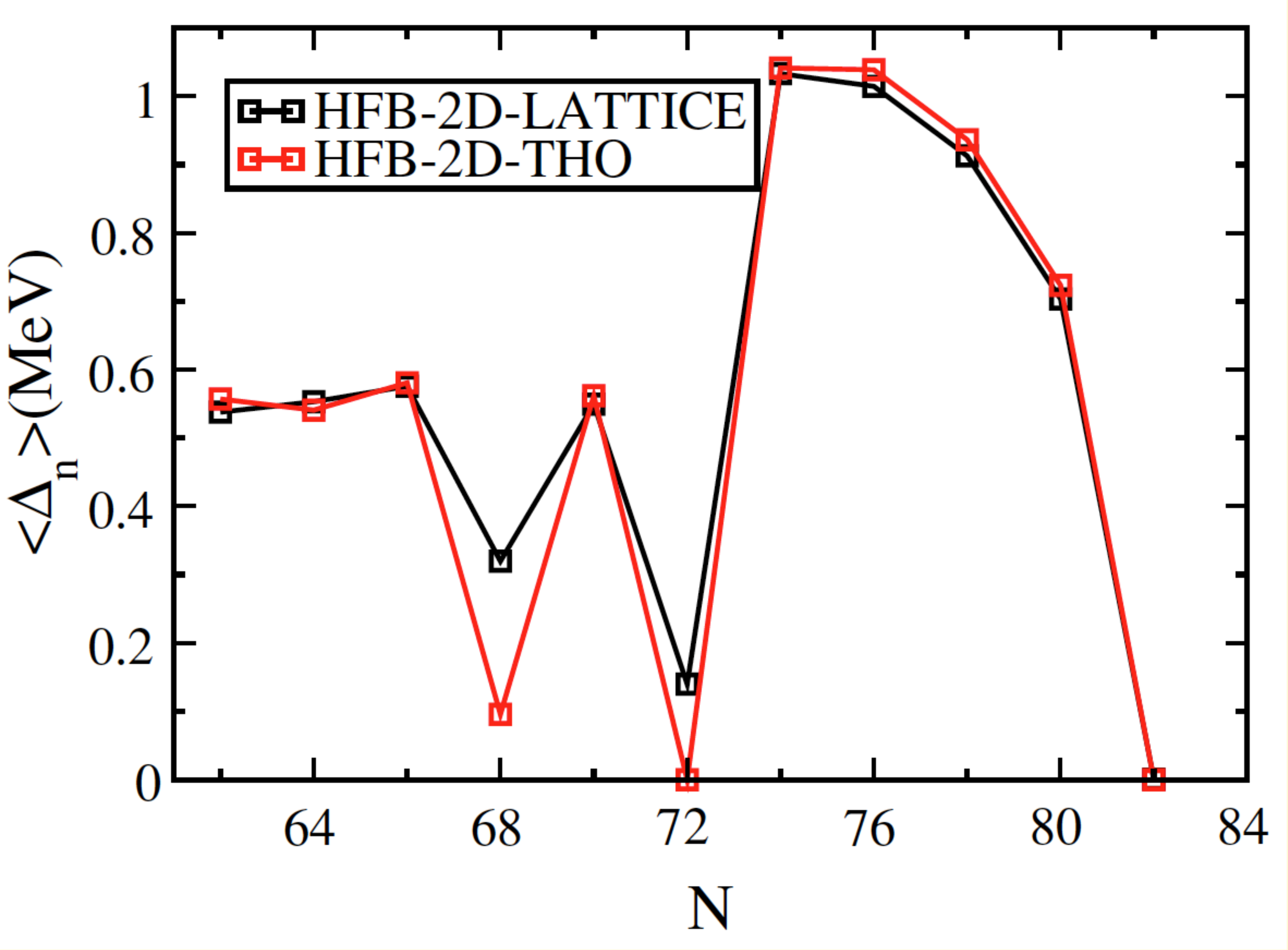

Zirconium isotopes (Z=40), HFB+SLy4 on 2D-grid

Blazkiewicz, Oberacker, Umar & Stoitsov, Phys. Rev. C71, 054321 (2005)

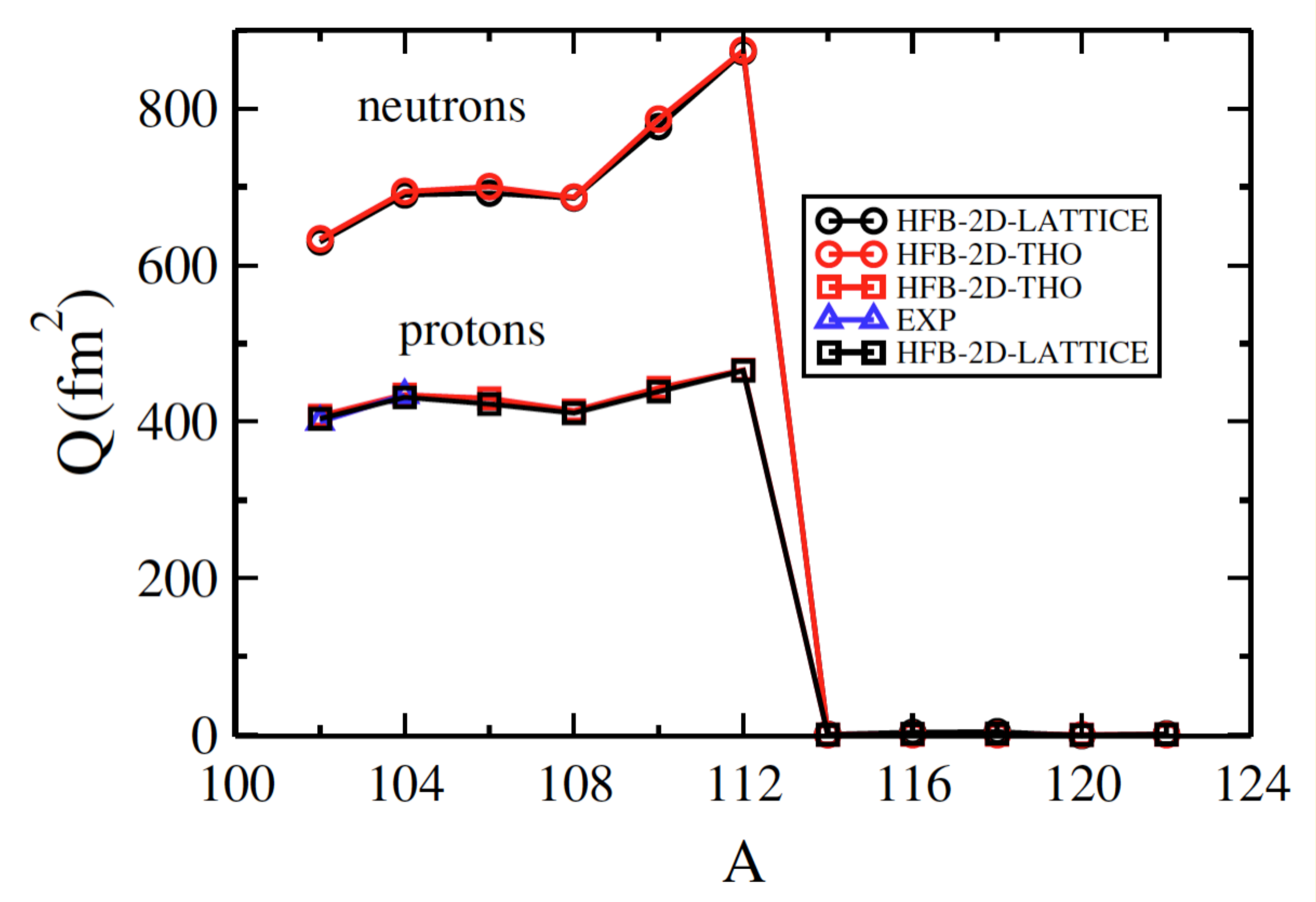

Tin isotopes (Z=50), HFB-1D for several Skyrme interactions

RIA Theory Bluebook (Sep. 2005), calculations by Dobaczewski et al.

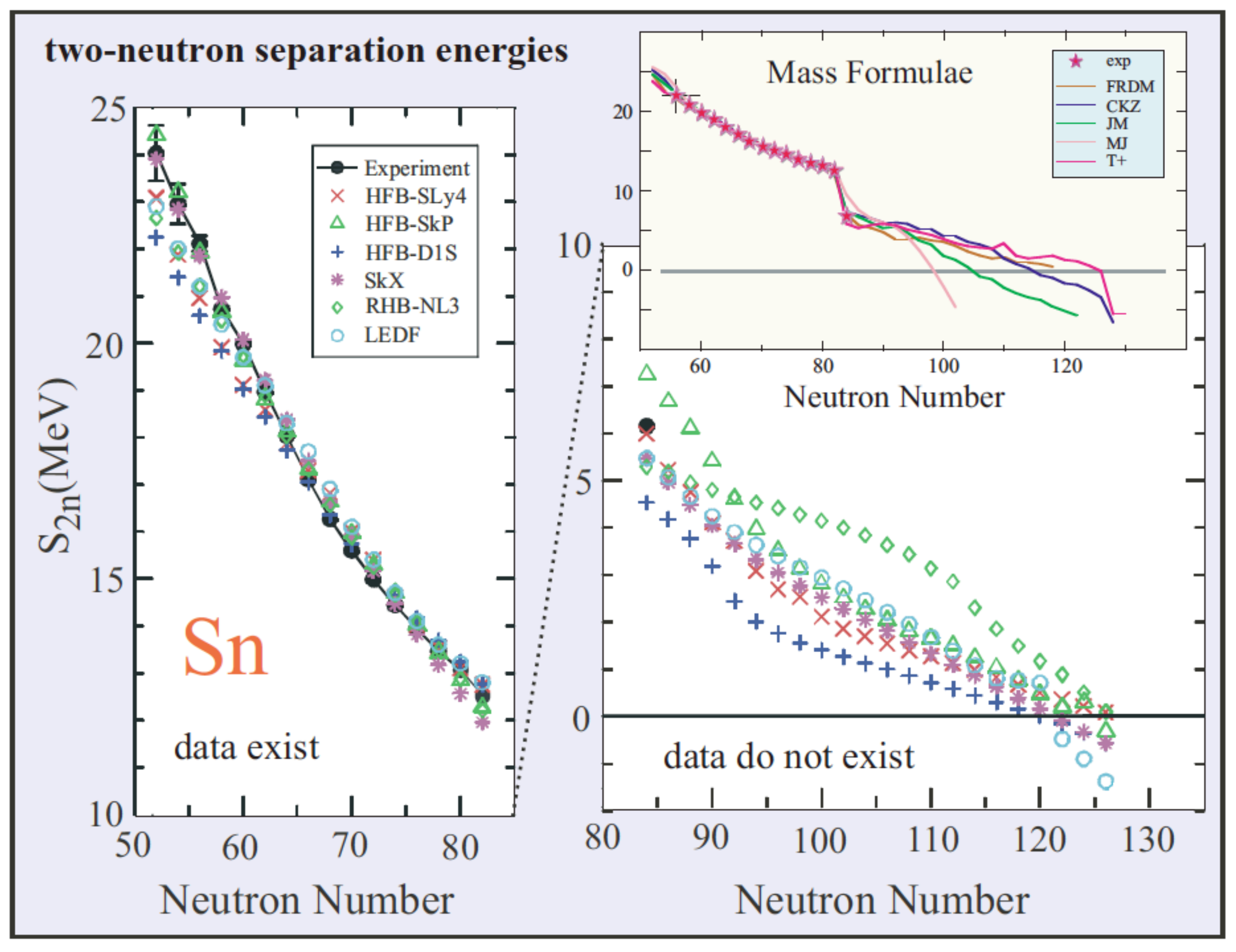

2-neutron separation energies (2-D HFB)

Dobaczewski, Stoitsov & Nazarewicz (2004) arXiv:nucl-th/0404077

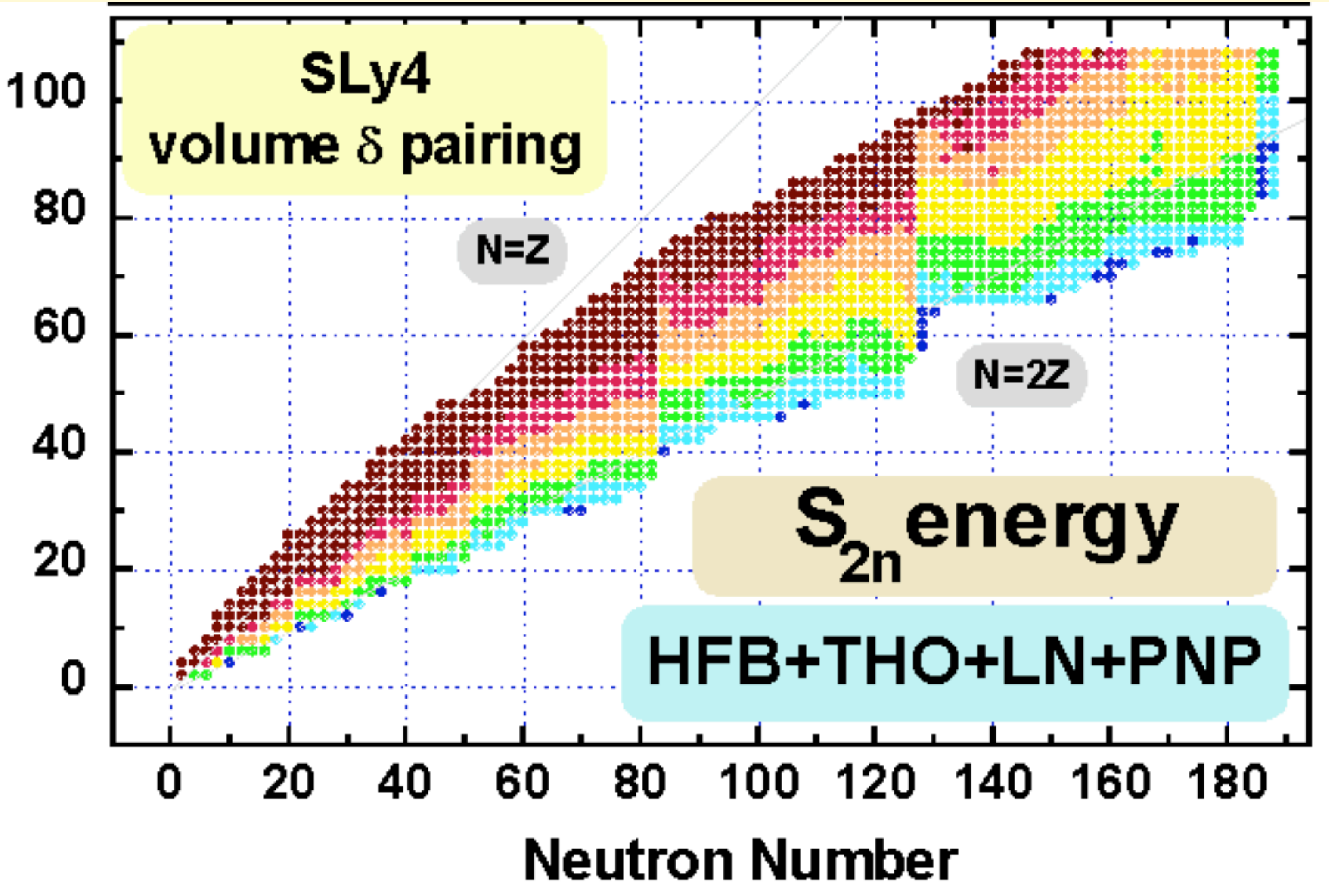

Nuclear ground state deformations (2-D HFB)

Dobaczewski, Stoitsov & Nazarewicz (2004) arXiv:nucl-th/0404077

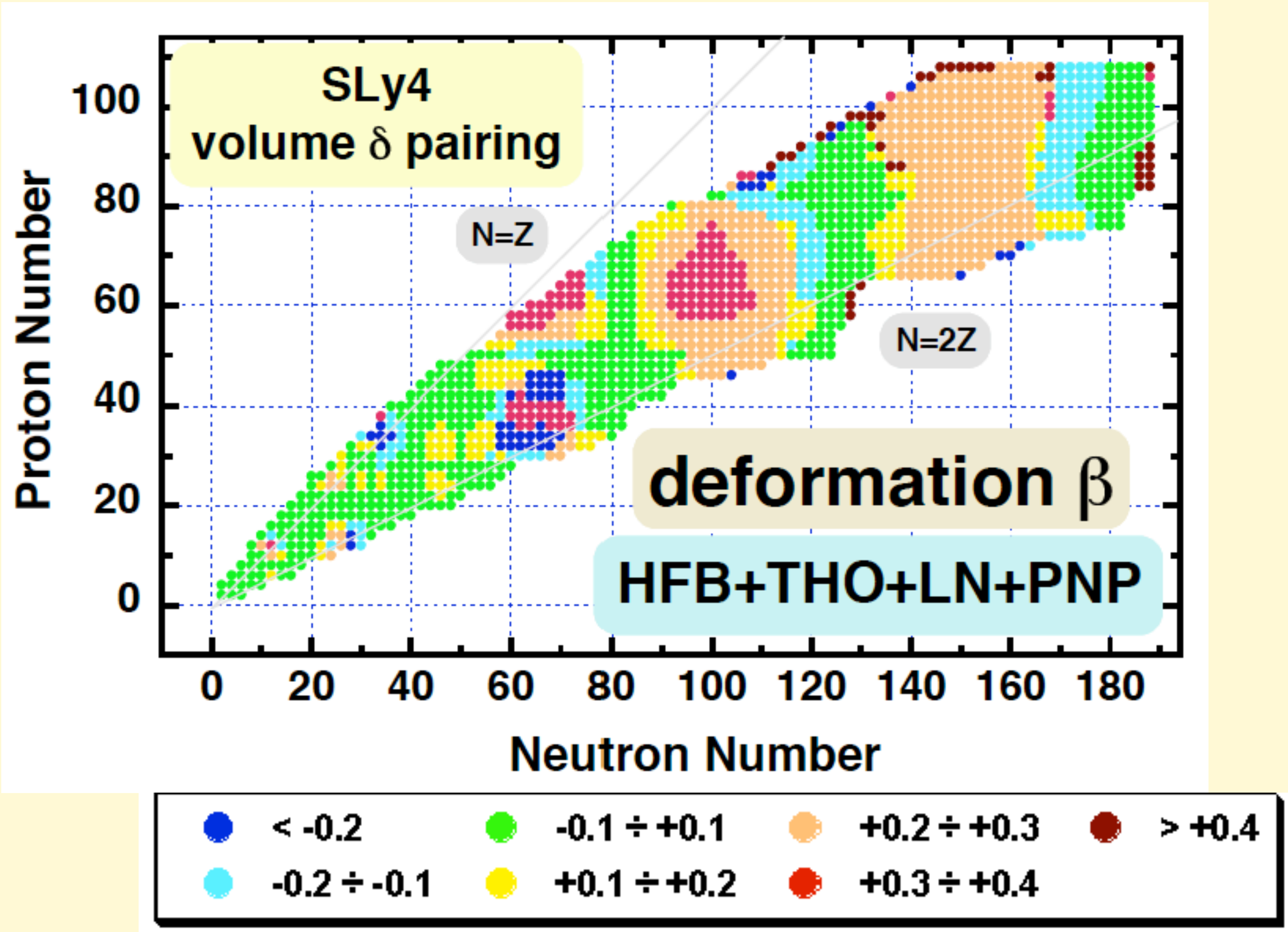

HFB with quadrupole + octupole constraints

H. Goutte, P. Casoli, and J.F. Berger, Nucl. Phys. A734 (2004) 217

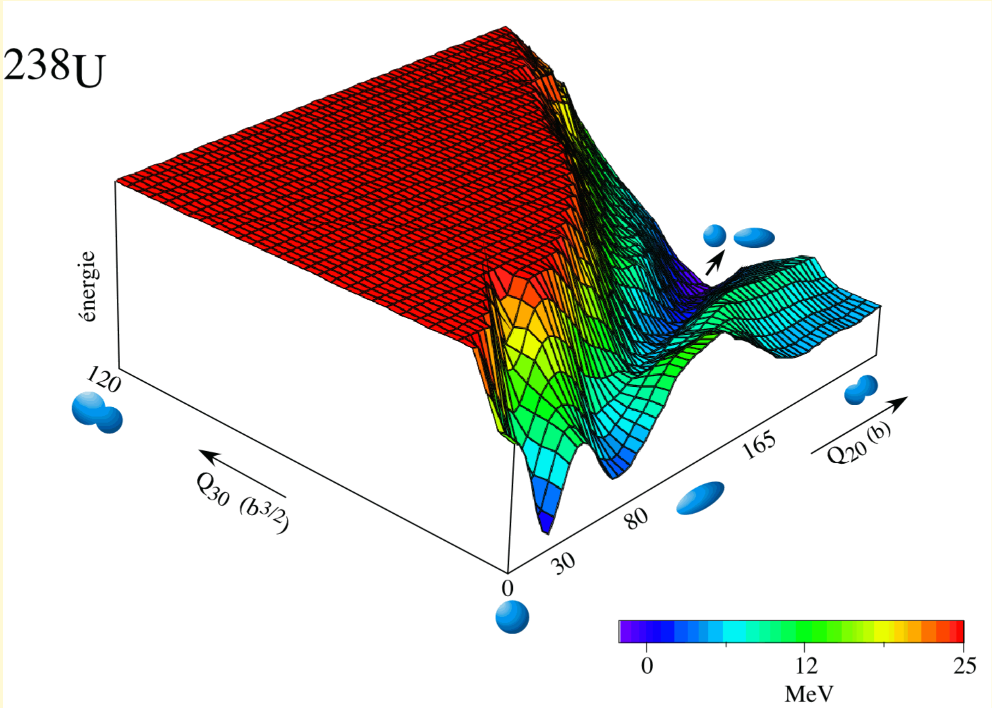

microscopic potential energy surface $E(Q_{20}, Q_{30})$ for nuclear fission:

Q_{20} – elongation

Q_{30} – mass asymmetry

Notice double-humped fission barrier in Q_{20} – direction !

HFB with quadrupole + octupole constraints

Robledo, Baldo, Schuck, and Viñas, Phys. Rev. C 81, 034315 (2010)

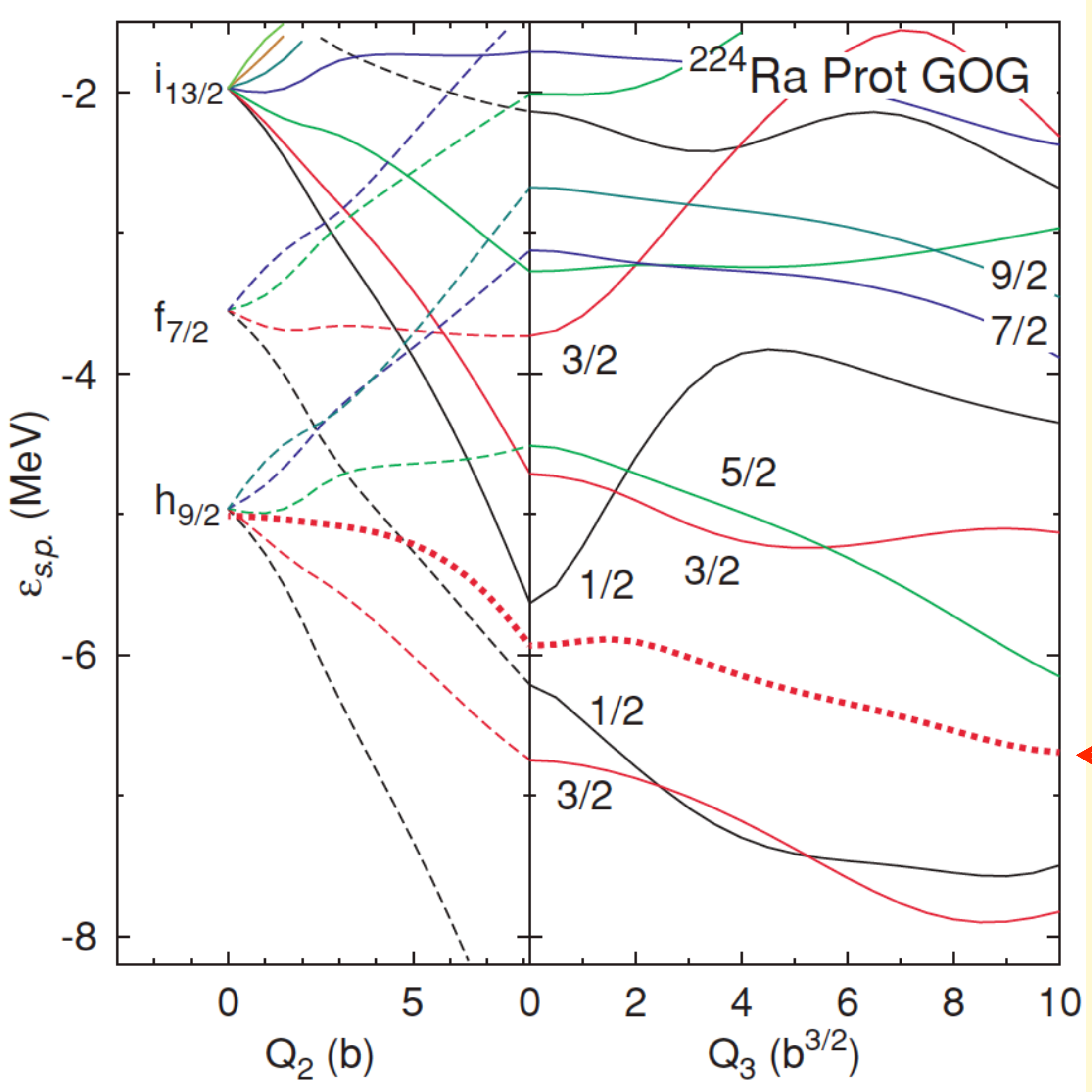

single-particle energies for proton levels in ^{224}Ra, as a function of

Q_2 – mass quadrupole moment

Q_3 – octupole moment

Total g.s. energy minimum at Q_2 = 8.12 b, Q_3 = 4 $b^{3/2}$

Constrained HFB calculation with Gogny effective N-N interaction.

Fermi level

Quenching of nuclear shell structure in neutron-rich nuclei

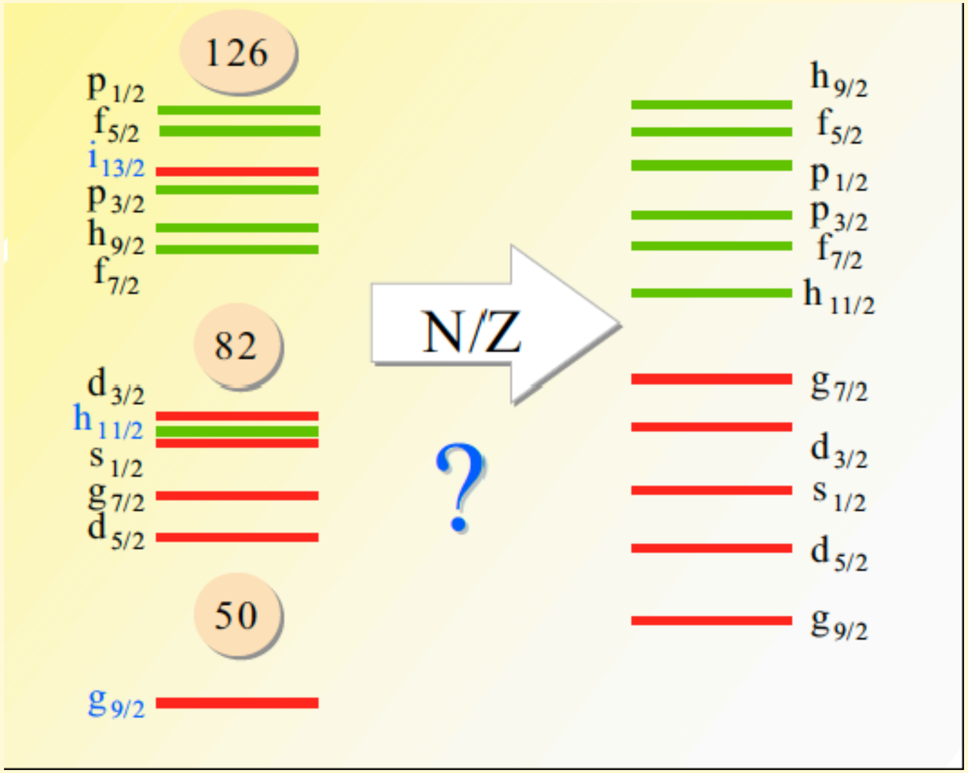

near stability line:
pronounced shell gaps

n-rich nuclei : shell gaps
suppressed due to
reduced LS coupling

Solar r-process: cosmic element abundance

RIA 2000 Whitepaper